Departement für Kleintiere, Abteilung für Radio-Onkolgie
der Vetsuisse-Fakultät Universität Zürich

Arbeit unter wissenschaftlicher Betreuung
von Prof. Dr. med. vet. Carla Rohrer Bley, Leitung Abteilung für Radio-Onkologie

Novel hyperthermia applicator system allows adaptive treatment planning: preliminary clinical results in tumor-bearing animals

Inaugural-Dissertation

zur Erlangung der Doktorwürde der
Vetsuisse-Fakultät Universität Zürich

vorgelegt von

Susann Dressel

Tierärztin
von Stollberg, Deutschland

genehmigt auf Antrag von

Prof. Dr. med. vet. Carla Rohrer Bley, Referentin

2017

Departement für Kleintiere, Abteilung für Radio-Onkolgie
der Vetsuisse-Fakultät Universität Zürich

Arbeit unter wissenschaftlicher Betreuung
von Prof. Dr. med. vet. Carla Rohrer Bley, Leitung Abteilung für Radio-Onkologie

Novel hyperthermia applicator system allows adaptive treatment planning: preliminary clinical results in tumor-bearing animals

Inaugural-Dissertation

zur Erlangung der Doktorwürde der
Vetsuisse-Fakultät Universität Zürich

vorgelegt von

Susann Dressel

Tierärztin
von Stollberg, Deutschland

genehmigt auf Antrag von

Prof. Dr. med. vet. Carla Rohrer Bley, Referentin

2017

Inhaltsverzeichnis

Vetsuisse Faculty, University of Zurich (2017)

Susann Dressel

Departement for Small Animals: Division of Radiation Oncology
Office: ehuber@vetclinics.uzh.ch

Novel hyperthermia applicator system allows adaptive treatment planning: preliminary clinical results in tumor-bearing animals

Abstract

Hyperthermia (HT) as an adjuvant to radiation therapy (RT) is a multimodality treatment method to enhance therapeutic efficacy in different tumors. High demands are placed on the hardware and treatment planning software to guarantee adequately planned and applied HT treatments. The aim of this prospective study was to determine the effectiveness and safety of the novel HT system in tumor-bearing dogs and cats in terms of local response and toxicity as well as to compare planned with actual achieved data during heating. A novel applicator with a flexible number of elements and integrated closed-loop temperature feedback control system, and a tool for patient-specific treatment planning were used in a combined thermoradiotherapy protocol. Good agreement between predictions from planning and clinical outcome was found in 7 of 8 cases. Effective hyperthermia treatments were planned and verified with the novel system and provided improved quality of life in all but one patient. This individualized treatment planning and controlled heat exposure allows adaptive, flexible and safe HT treatments in palliatively treated animal patients.

Keywords: hyperthermia, adaptive treatment planning, radiation, dogs, cats

Vetsuisse-Fakultät Universität Zürich (2017)

Susann Dressel

Departement für Kleintiere: Abteilung für Radio-Onkologie
Sekretariat: ehuber@vetclinics.uzh.ch

Novel hyperthermia applicator system allows adaptive treatment planning: preliminary clinical results in tumor-bearing animals

Zusammenfassung

Hyperthermie in Kombination mit der Strahlentherapie gilt als eine multimodale Behandlungsmethode um den therapeutischen Effekt in verschiedenen Tumorarten zu steigern. Hohe Anforderungen werden an die Hardware und Behandlungssoftware gestellt, um eine adäquat geplante- und applizierte Hyperthermiebehandlung zu gewährleisten. Die Ziele dieser prospektiven Studie beinhalten die Effektivität und Sicherheit des neuen Hyperthermiesystems in acht caninen und felinen Tumorpatienten hinsichtlich der lokalen Therapieansprache und Toxizität zu testen und die geplanten mit den applizierten Behandlungsdaten während des Heizvorganges zu vergleichen. Ein neuer Hyperthermie Applikator, welcher aus einer flexiblen Anzahl von Elementen besteht und ein integriertes thermisches Feedback-system enthält, sowie eine patienten-spezifische Planungssoftware wurden in einem kombinierten Thermoradiotherapie Protokoll verwendet. Gute Übereinstimmungen zwischen den Vorhersagen der Therapieplanung mit den klinischen Ergebnissen wurden in 7 von 8 Fällen gefunden. Effektive Hyperthermiebehandlungen konnten mit dem neuen System geplant und angewandt werden und führten zu einer verbesserten Lebensqualität in allen bis auf einen Patienten. Die Kombination aus der individuellen Behandlungsplanung und der kontrollierten Wärmeübertragung liefert eine adaptive, flexible und sichere Hyperthermiebehandlung von palliativ behandelten Tierpatienten.

Schlüsselwörter: Hyperthermie, adaptive Therapieplanung, Strahlentherapie, Hunde, Katzen

Introduction

Hyperthermia (HT) in conjunction with radiation therapy (RT) has long been employed as a method to increase therapeutic efficacy in certain tumors.[1-6] The uniform application of heat to a localized tumor is difficult to achieve due to the inhomogeneous anatomy with large dielectric contrasts, intra-tumoral tissue heterogeneity and physiologic counter-regulation, making the prediction or measurement of the temperature distribution demanding.[7-9] The application of HT places high demands on both the applicator hardware and treatment planning to guarantee accurate steering and an effective, safe therapy. Similar to RT systems, HT applicator systems should not only include the hardware component but also integrate a software component. i.e., suitable planning and control tools which allow predictive planning and steering of thermal dose administration. Accurate exposure control to prevent under-exposed target regions and unwanted hotspots in healthy tissue require a precisely controlled applicator system (amplitude and phase), precise spatial positioning of the applicators with respect to the patient body, high-resolution electromagnetic (EM) and thermal simulations considering at least the local anatomy and adequate tissue models (dielectric, thermal, perfusion).[10-12] Either a reliable prediction or a closed-loop system with thermometry-based feedback is needed to ensure a good correlation between planned (applied) dose and the effectively deposited heat in specific tissues over the time of treatment.

Over the last decade, progress has been made in terms of improved treatment accuracy and treatment planning guidance. Paulides et al.[13-15] showed that pre-treatment planning simulations and improvements in hardware elements (water bolus shape stability) as well as accurate patient positioning optimize the treatment quality in human head and neck cancer patients. Their approach involved 3D patient-specific EM and thermal simulations, which improve focused deposition of energy and enable conformal, reproducible and adaptive HT applications.

Thermal dose quantities are intended to enable a comparison of different treatments regarding biological effectiveness. This is not possible by a single temperature figure; instead, temporal changes and spatial temperature inhomogeneities should be taken into account.[16]

In the present prospective pilot study, we treated tumor-bearing companion animals in order to test the clinical use of a new multi-modular radio-frequency (RF) applicator system and treatment

planning tool for HT. By using EM, thermal, and induced effect simulations, the individual placement of applicators as well as their main parameters were optimized and temperature predictions were made. During treatment, temperature probes - implanted prior to the first treatment - supervised safe delivery, validated temperature predictions and allowed adaptation of energy delivery. For evaluating treatment intensity two different approaches, the CEM isodose concept and a transient thermal dose equivalent (TTDE) were used.[17]

The primary goal of our study was to test the applicability of the novel HT hard- and software components in clinical tumor-bearing dogs and cats, and to compare planned with actual achieved data during heating. As secondary endpoints, response to treatment was described with respect to observed toxicity and local tumor response in the treated animal patients.

Material and methods

HT treatment was performed using a novel applicator prototype (developed by the IT'IS Foundation, Zurich, Switzerland) with the possibility of grouping multiple elements to form an array with a flexible number and position of the elements, and an integrated closed-loop radiated electromagnetic field (EMF) feedback control system. Thermal delivery was prospectively planned with treatment-planning tool that was developed based on the computational life sciences platform Sim4Life (ZMT Zurich MedTech, Zurich, Switzerland). The treatment-planning tool was empowered to segment individual animal patients with iSEG (ZMT Zurich MedTech, Zurich, Switzerland), to semi-automatically optimize the placement of the applicator system, to determine personalized steering parameters using a dedicated field optimizer, and to perform analysis and visualization functionality. For the current investigation, feline and canine tumor animal patients with various types of inoperable cancers were included. In this experimental clinical setting, we used multiple temperature probes in order to validate the predicted intra-tumoral and superficial temperatures achieved during treatment. The measurement data obtained was then used to ensure that the applied treatment corresponds the predictions made during planning and allowed real-time adjustment in order to provide effective and safe heating.

Animal patient criteria

Dogs and cats presented to the Division of Radiation Oncology, Vetsuisse Faculty (University of Zurich, Switzerland) for treatment of inoperable bulky malignant tumors between July 2015 and August 2016 were included into the study. No preselection with regard to applicability of hyperthermia, e.g., based on modeling of the expected heating quality, was performed, resulting in an extremely heterogeneous group of animals with regard to tumor type, location, and heatability. Each animal had a clinical work up (tumor staging) as appropriate to the type of presenting disease. Written owner's consent was obtained for invasive sampling in this study. *The work was carried out in strict accordance with the recommendations and the protocol approved by the* Animal Ethics Council of the Canton of Zurich, Switzerland *(Permit Numbers: 172/13 and ZH065/16). All treatment and invasive sampling procedures were performed under anesthesia with appropriate analgesia, and all efforts*

were made to ensure minimized suffering.

Hyperthermia and radiotherapy treatment planning

A treatment planning computed tomography (CT) was acquired in an individually prepared immobilization device: animals were positioned in a vacuum cushion (BlueBag BodyFix, Elekta AB, Stockholm, Sweden) and a custom-made bite block was used, if required[18]. Immobilization also served the purpose of achieving reproducible positioning and to align planning and treatment. A non-contrast and contrast-enhanced study was performed to visualize the tumor. Subsequently, temperature transponder seeds (IPTT-300, Bio Medic Data Systems, Inc., Seaford, USA) were implanted in a minimally invasive manner in viable tumor areas, avoiding cystic or necrotic regions, which are likely to result in sensor migration. After implantation, an additional CT study was performed to confirm the transponder location. Both, the initial CT (without transponders) and the post-injection CT (with transponders) were later used for segmentation.

RT treatment planning was performed in all cases by a board-certified radiation oncologist (CRB) on the basis of 3D CT data using the Eclipse External Beam Planning system version 10.0 (Varian Oncology Systems, Palo Alto, USA). Tumor related volumes were contoured as follows: the gross tumor volume (GTV) was delineated using co-registered contrast-enhanced CT sequences; the clinical target volume (CTV), accounting for subclinical microscopic disease extension, was defined according to the radiation oncologist's choice for the respective disease; and, based on tumor location, the CTV-PTV margin extension was a three-dimensional extension by 2-5 mm to define the planning target volume (PTV), accounting for systematic and random uncertainties. Organs at risk were specified as required.

For HT treatment planning, the CT images and the previously defined tumor (GTV) and organs at risk related volumes from the RT treatment planning (RTstruct DICOM images) were imported into iSEG. This segmentation toolbox features a set of flexible (semi-) automatic segmentation methods enabling to generate a detailed 3D-anatomical model distinguishing the large number of tissues required for HT treatment planning.[19] Basic tissue types were identified based on anatomical criteria and Hounsfield units obtained from the non-contrast and contrast-enhanced

treatment planning CT. Additional segmentation functionality was used to semi-manually delineate relevant organs or organs at risk (e.g. spinal cord, bone marrow, liver, kidney) that were not clearly distinguishable by their contrast, however vary in their physical, dielectric and thermal properties. The segmented tissues were later assigned physical (i.e., mass density), dielectric (i.e. electric conductivity and permittivity), and thermal (i.e. thermal conductivity, specific heat capacity, heat generation rate, and temperature dependent perfusion) tissue properties.[20] In order to know their position, the temperature sensors (see below) were also included in the segmentation, allowing prediction of temperature recordings during treatment. Subsequently, the treatment-planning enhanced Sim4Life platform was used for surface generation and visualization of the segmented anatomical model to then plan optimized therapy administration. EM and thermal simulations were performed to identify the optimal number of applicators, their placement and polarization, the water-bolus/boluses temperature, as well as the applicator parameters (i.e. phase and amplitude of delivered fields). Geometrical placement of the applicator was interactively defined, with the possibility of automatically generating 3D printable fixation mask. Alternatively, simple dielectric supports could also be generated to fix the applicators in their final position. EM simulations were performed using a finite-difference time-domain (FDTD) solver to compute the full-wave solution of Maxwell's equations. A modified version of the Pennes Bioheat Equation (PBE) with advanced perfusion and thermoregulation modeling accounting for vasodilation was used for the temperature simulations. The temperature dependency of the perfusion in the tumor,[21] muscle, fat and skin[22, 23] was modeled and considered in all the simulations. Effect-related thermal dose quantities such as isopercentiles of temperature or *CEM*43 (cumulative equivalent minutes at 43˚C)[16] were computed, analyzed, and displayed providing, e.g., a visualization of the effective treatment volume with an overlay of the efficacy/risk maps, or systematic assessment of tumor coverage and sensitive tissue exposure through cumulative histograms.

Applicator

The newly designed applicator prototype (Figure 1) consists of different elements, including a cavity-backed slot antenna,[24] operating in the industrial, scientific, and medical band at 433.92 MHz, positioned around or near the region to be treated. The design of the applicator offers full flexibility

with respect to the location at which the applicator can be placed, the orientation, and the number of applicators to be used for the treatment.[25] Different paradigms can be used depending on tumor location, namely, coherent (phased-array) or incoherent (specific absorption rate (SAR)) combining techniques, to raise the temperature of the tumor by focusing energy into it. Cavity-backed slot antennas are chosen for this application because of their wide bandwidth and hence tolerance to changes in environment ('loading conditions'), such as proximity to the patient, tissue parameters, and morphology. A technique based on sensing the radiofrequency (RF) current flowing in each of the applicator elements is employed to determine the amplitude and phase of the total field radiated due to both direct and coupled excitations of the elements, and hence provides a measure in terms of SAR of the power absorbed by the tissues. The measurement is performed by an integrated data acquisition system. The applicator elements have an overall external area of 75 mm x 75 mm. The effective heat transfer coefficient of the water boluses was determined experimentally and applied subsequently in the thermal simulations as a convective boundary condition.

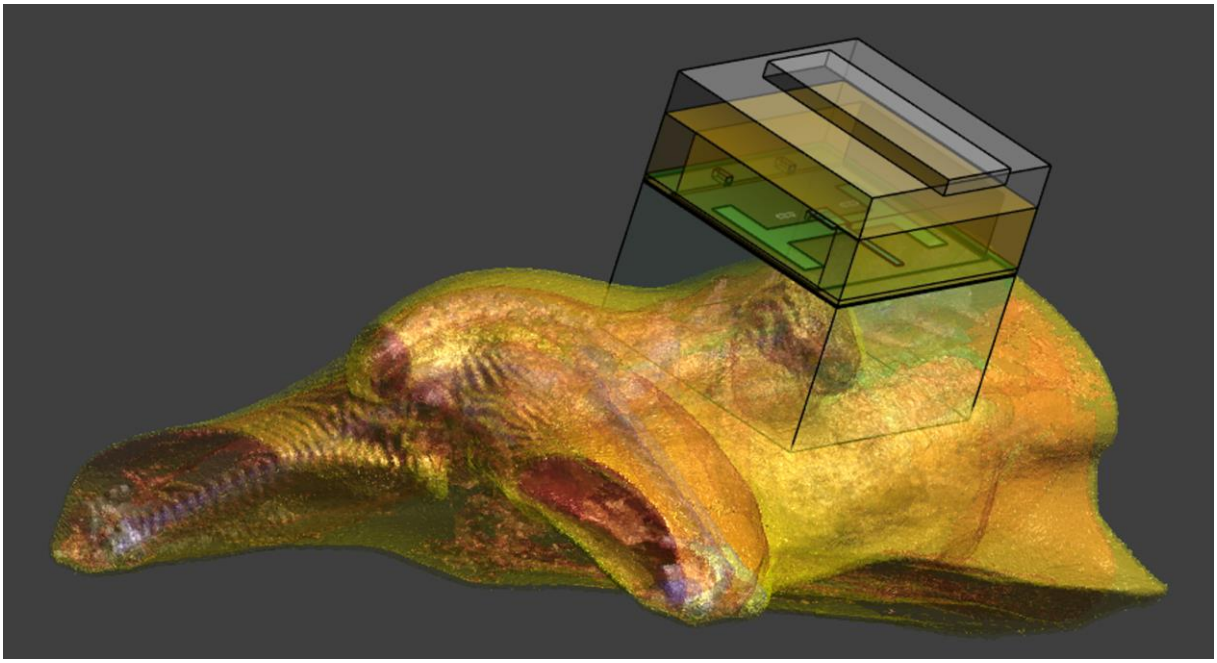

Figure 1. Picture showing the 3D view window of the treatment-planning tool with the optimized placement of one of the novel applicator modules on the tumor of a cat (animal 6). In this case, the vaccine-associated sarcoma is located on the right caudodorsal abdominal wall. (only the caudal abdomen and pelvic region relevant for reliable modeling is segmented)

Hyperthermia treatment

HT was performed once per week for three sessions in total, in each case prior to RT. All animal patients were under general anesthesia and positioned in the individually shaped vacuum cushion and, if treated in the head area, a bite block, providing rigid immobilization and reproducibility of treatment position, compared to the planning position. An array of between one and six RF-applicators with individual water-filled boluses can be applied around a localized tumor, according to the individual treatment plan. In order to avoid the gross mismatch that can occur when an applicator operates with air between the bolus and patient, fur over the treated region was clipped and additional absorbing material (saline-solution filled bags) was placed around the tumor, if required, to fill air voids present due to the shape of the anatomy. If the skin of the tumor was ulcerated, the treated region was covered with cling film to avoid contamination.

Effective heating time was 45 minutes, measured from the time when the first intra-tumoral temperature sensor reached ≥41°C, or after 15 minutes of heating-up time had elapsed. In the clinical setting, the target tumor temperature was between 41°C and 44°C throughout treatment. Superficial skin temperatures were supposed to remain below 42°C. Intra-tumoral temperature was monitored with the implanted temperature sensors. Depending on tumor size, two to three sensors were placed in the tumor under CT-guidance, subsequently remaining at the implanted site. The transponders were placed in tumor regions with the greatest possible distance to each other, to enable optimal temperature measurement coverage and readability. Temperatures were evaluated every 5 min with a handheld device (DAS-7009 IPTT, Bio Medic Data Systems, Inc., Seaford, USA). For each reading, the applicators and boluses had to be removed from the animal. Surface temperatures were continuously monitored with a non-invasive T1V3 temperature probe connected to the EASY4 data acquisition system (Schmid & Partner Engineering, AG, Zurich, Switzerland), which was placed between the water bolus and the skin.

To quantify the treatment intensity of applied heat, thermal dosimetry was used, meaning that the temperature as function of time was translated into a biological effect. It is important to note that thermometry alone is not sufficient to achieve this; the temperatures acquired with thermometry need to be transformed into thermal doses. Thermal dose was calculated for each temperature sensor and

was converted to an equivalent exposure time in minutes at a reference temperature of 43°C, using the following formula from Sapareto and Dewey:[16]

$$CEM43 = \sum R^{(43-T)} \Delta t \text{ (min)}$$

where Δt was 5 min (the time between readouts of the implanted sensors), T is the applied temperature of the target tissue and R= 0.25 when T ≤43°C and R = 0.5 when T >43°C.

Since a physiological thermal dose concept is missing up to now, an alternative approach for TTDE was investigated in addition to the *CEM*43 dose. It is based on a physiologically motivated model,[17] in which the total amount of repair protein is divided into two parts: The amount of nonfunctional repair protein Λ and the amount of functional repair protein $\Upsilon = 1 - \Lambda$. Λ is a dynamic quantity that rises during heating and decays subsequently due to repair processes. The change in functional repair protein amount then consists of the amount of non-functional repair protein that becomes functional minus the amount of functional repair protein that becomes non-functional:

$$\frac{\mathrm{d}\,\Lambda(t)}{\mathrm{d}t} = k_1\,\Upsilon(t) - k_2\,\Lambda(t)$$

First order kinetics are assumed; the coefficient k_1 is given by the Arrhenius equation

$$k_1 = \kappa e^{-E_a/(RT)} \text{ with } \kappa = a \cdot e^{E_a/(RT_{ref})}$$

where $R = 8.314$ J mol^{-1} K^{-1}, T is the temperature in [K] and t is the time. A constant parameter $k_2 = 2.76$ h^{-1} is assumed. The pre-exponential factor of the Arrhenius equation κ consists of $a = 0.56 \cdot 10^{-3}$ h^{-1} and a factor introduced for numerical reasons with $T_{ref} = 310.15$ K. The activation energy is set to $E_a = 1528$ kJ/mol. Those values were found by fitting the data presented by Sapareto and Dewy,[16] and were published by Scheidegger et al.[17] Note how this model does not incorporate the change of activation energy when the temperature exceeds 43˚C, unlike the behavior postulated by the *CEM*43 model. The initial condition is derived from the steady-state at standard body temperature, is $\Lambda(0) = k_1/(k_1 + k_2) \approx 0$.

Λ is evaluated at two points in time for two thermal dose candidates: the first one is the maximum amount of nonfunctional repair protein during the procedure, Λ_{max}. The second one, Λ_{gap}, is the amount of nonfunctional repair protein at the time of irradiation t_{RT}, taking into account the time-gap between HT and RT.

Radiation therapy

RT was applied after HT while trying to keep the time gap between the two treatment modalities as short as possible. Time from shutting-off the RF-power to applying the first radiation beam was recorded for each animal and treatment. RT was delivered with a 6 megavolt (MV) linear accelerator (Clinac iX, Varian, Palo Alto, USA) using photons and a 3-dimensional conformal technique. The recommendations for specifying dose and treatment volumes as proposed for veterinary medicine were adhered to.[26-28] The protocols used correspond to commonly used protocols for palliative treatment in animals. For sarcoma, a total of 30 Gy delivered in five fractions of 6 Gy applied twice per week (as shown in Figure 2), resulting in an overall treatment time of 2.5 weeks.[29] For oral melanoma, a total of 32 Gy was prescribed and delivered in 4 x 8 Gy weekly.[30, 31]

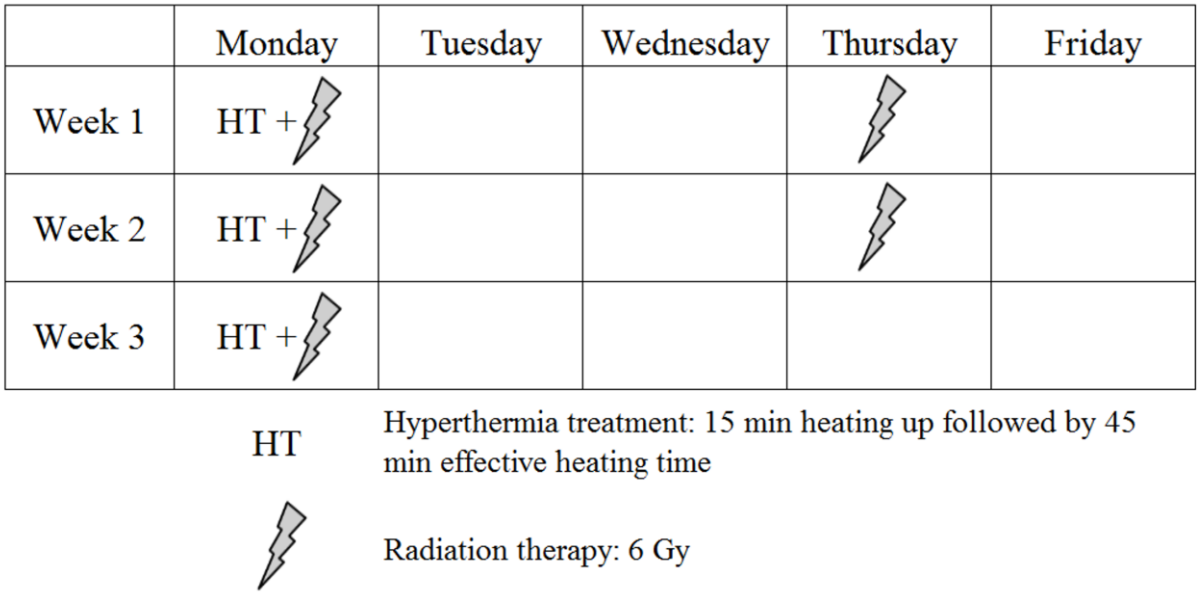

Figure 2. Graphical illustration of a 5 x 6 Gy radiation therapy protocol in combination with hyperthermia used for the treatment of soft tissue sarcoma.

Response evaluation and follow-up

After treatment, animals were re-evaluated after three weeks, two, three, four and six months and then at three-month intervals. Follow-up information included physical examination with measurement of the tumor and individualized imaging based on tumor type, stage and clinical signs. A modified Karnofsky´s performance score[32] was performed before treatment initiation, during HT treatments and regular re-checks. Pre- and post-treatment tumor volumes were extracted with the contouring tool of

the Eclipse External Beam Planning system version 10.0 (Varian Oncology Systems, Palo Alto, USA) or by the manual calculation of an ellipsoid ($V = \pi / 6$ x (L x W x H)) using caliper and / or CT-measurements. On the last treatment day as well as no later than six months after the end of the treatment, a CT of the tumor region was performed and was repeated every six months thereafter. Tumor response was evaluated, based on size measurements, using the response evaluation criteria in solid tumors (RECIST) for dogs.[33]

At time of progression, animal patients were allowed to receive additional treatment (e.g. metronomic chemotherapy or surgical debulking). Radiation-induced toxicity was scored using the Veterinary Radiation Therapy Oncology Group (VRTOG) scheme each time RT was applied, and at regular re-checks.[34] Hyperthermia-specific side effects were graded according to the Common Toxicity Criteria Adverse Events (CTCAE) v4.03[35] and Quality Management in Hyperthermia (QMHT)[35] on each treatment day and on all follow-up examinations.

Statistical analysis

Data was compiled in Excel (Microsoft, Redmond, USA).

Descriptive statistics are reported on the following variables: (1) pre-treatment longest tumor diameter, (2) maximum reduction of the longest diameter after treatment, (3) reduction in tumor volume, (4) time to greatest response and (5) median skin temperature during treatment, as well as on the three thermal dose candidates (6) $CEM43$, (7) Λ_{max}, and (8) Λ_{gap}.

Progression free interval (PFI) was defined as the interval between the first hyperthermia treatment to measurable local or distant tumor progression. Overall survival (OS) was defined as the time between the first hyperthermia treatment and death from any cause. Follow-up time was defined as time between the first hyperthermia treatment and the last re-check or death.

Results

Animal patient and tumor characteristics

Eight client-owned companion animals were included into a combined thermoradiotherapy protocol receiving in total three sessions of HT as an additive to hypofractionated RT.

Animal and tumor characteristics are summarized in Table 1. Two animals were treated with a deviating RT protocol: in one dog (animal 1) a smaller fraction size was used with the initial plan to downstage the tumor and render it amenable to surgery. A total dose of 36 Gy, applied in 12 x 3 Gy (daily fractions) was given. Animal 3 had been pretreated 15 months earlier with a 5 x 6 Gy palliative protocol and for the re-treatment a more conservative approach of 3 x 5 Gy, applied concurrently with the three weekly HT treatments was used.

Hyperthermia treatment parameters

Results obtained from treatment planning provided guidance for setting up the starting parameters during the therapy, namely the applicators position and polarization, the power (amplitude and phase) of the RF signal for each applicator, and the temperature of the water flowing within the bolus. Because of the intrinsic uncertainties and approximations in modeling the treatment (heterogeneous distribution of blood flow in actual GTV, accuracy of anatomical model, uncertainties about EM and thermal properties of the tumor, transponder migration from injection time to each session, applicator positioning), real time power strength adjustments based on the measured temperatures of the transponders (see also Figure 3) and the instantaneous temperature readouts of the skin were performed: in total, 490 intra-tumoral temperature readouts were conducted during the effective heating period in all animals, 320 (65 %) of them were within the range of 41 – 44°C. The power had to be adjusted with a mean of 4.25 times (± 2.2 times) during the treatments. Skin temperature was measured continuously whenever possible (available in 15 out of 24 treatments) to avoid excessive heating (>42°C). In six treatments (animals 6, 7, 8) skin temperature was elevated above this target for between 4.47 and 49.67 minutes (median 11.0 min) to allow therapeutic tumor temperatures. Simulated times to reach therapeutic temperatures were always shorter than those required in reality as the need to stop the treatment to read the implanted temperature sensors lead to a drop in tumor

temperatures. Hence, the overall treatment time (heating up + effective heating time + temperature readouts) took in 17 (71 %) out of 24 cases more than the desired 60 min. The mean time to reach intra-tumoral temperatures ≥41°C in at least one temperature sensor was 15 min (± 8 min) and in one case (animal 7) the target temperature was not achieved during the entire treatment. In cases where the target therapeutic temperatures were not reached within the intended heating-up time (n = 5), therapeutic time was still initiated to avoid prolonging anesthesia of the animals. Mean heating-up time in all treatments was 13.1 min (± 5.4 min) and the mean effective heating time (power turn-offs included) was 52.4 min (± 7.0 min). Mean time between HT and RT treatment was 21.6 min (± 8.4 min), deviations occurred due to positioning verifications of the animals before RT treatment.

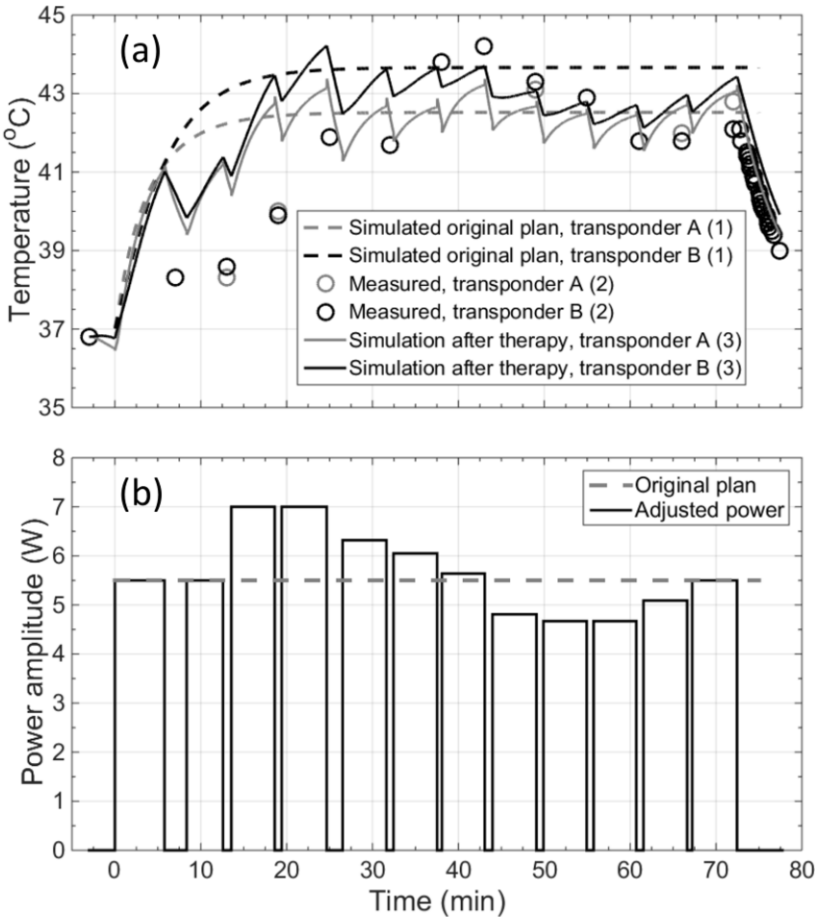

Figure 3. Comparison between planned and applied treatment for one treatment of animal 6. (a) Simulated and measured temperatures inside the tumor as a function of time: (1) the original optimized treatment plan using a constant power strength, (2) the actual temperatures obtained from the transponders every 5 min, including the temperature drop at the end of the therapy for one of the transponders, and (3) simulation after therapy application, considering the variation of applied power during the therapy and the exact time slots when the power was turned off and the water bolus was removed (i.e. the periods in which the temperature from the sensors was acquired). (b) Power applied to the applicator as a function of time according to the original treatment plan and the actually applied, dynamically adjusted (based on temperature sensors) power during the session.

Expected and measured temperatures, as well as the computed and applied power in the applicator as a function of time for one of the treatments of animal 6, are displayed in Figure 3. In the transient region (i.e., the region in which the temperature changes with time before reaching a steady state), the measured temperatures were approximately 2°C below the predicted value, even considering the actual power and bolus absence. Besides the EM and thermal parameter uncertainties, the deviations can be attributed to uncertainty about dielectric, thermal, and perfusion properties of the various tissues, and especially the heterogeneous tumor region. Additionally, literature data on the temperature dependence of the tumor perfusion is sparse and important variability exists between tumor types, such that the applied perfusion model also contributes to the uncertainty. Nevertheless, the main impact on the temperature response was a prolongation of the transient regime. In the steady state, the deviations between the measured values and both, the original plan and the realistic simulation, were considerably decreased. The temperatures acquired by the transponders during each treatment give some indication of the uniformity of heating. Table 2 shows the minimum and maximum intra-tumoral temperatures measured by the transponders during the effective heating time for each therapy session. This range indicates how uniformly the tumor was heated over time, after reaching the temperature criteria for hyperthermia. The same table summarizes the main parameters for all animals at each therapy session (number of applicators, initial power amplitude and water bolus temperature). A useful metric for evaluating the quality of a planned treatment is the volume-normalized temperature histogram. The histogram allows estimation of the temperature uniformity inside the tumor, but also indicates for this study that sensitive tissues (e.g. the spinal cord) were within a safe temperature range. Figure 4 shows the corresponding temperature histograms for the GTV and the spinal cord, respectively, for animal 6. As illustrated, 74 % of the tumor volume is expected to reach at least 41°C, 44.6°C being the maximum temperature. On the other hand, the spinal cord is expected to always remain below 39.3°C.

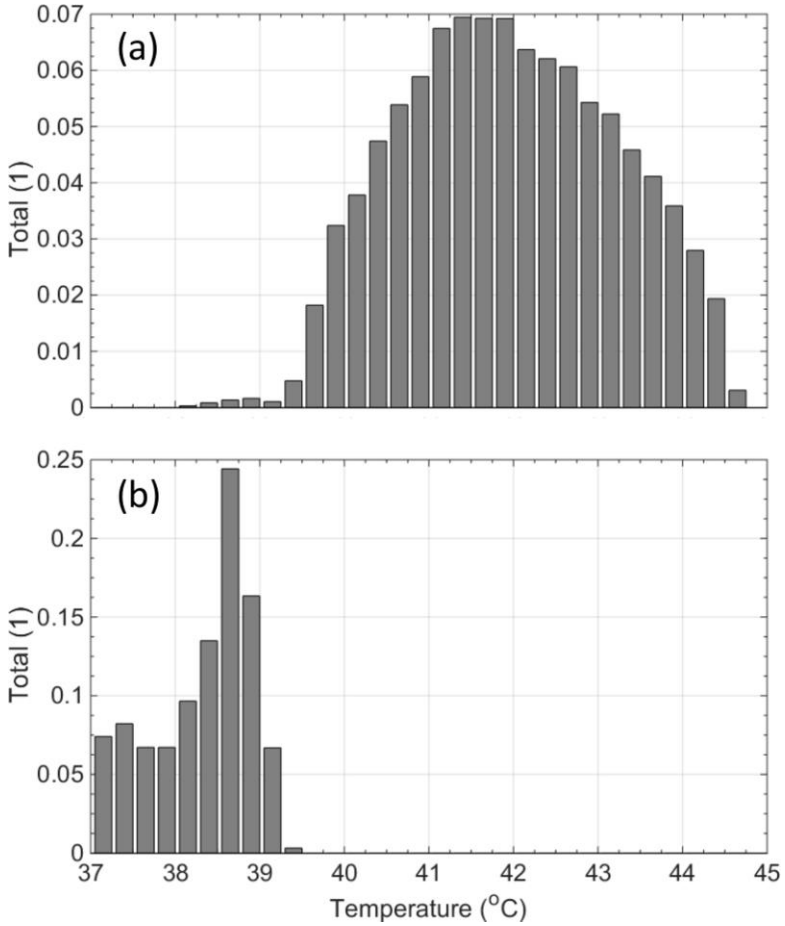

Figure 4. Temperature histograms for (a) the GTV and (b) the spinal cord in animal 6. In the case of the tumor, 74% of its volume is expected to reach at least 41°C, 44.6°C being the maximum temperature. The spinal cord temperature is expected to always remain below 39.3°C.

Typical metrics for assessing the homogeneity of heating inside the tumor are T90 and T10, defined as the temperature reached by at least 90 % and 10 % of the tumor volume, respectively. The cumulative histogram for the GTV is used in the treatment planning to calculate the T90 and T10 factors, as summarized in Table 2 for all the animals. The difference $\Delta T = T10 - T90$ gives an indication of the uniformity of heating inside the tumor; a smaller ΔT indicates a more uniform heating. It should, however, be noted that uniform heating alone does not guarantee that the tumor reaches therapeutic temperatures. A valuable predictor of treatment efficacy is provided by ascertaining a T90 close to or above 41°C. This last criterion was fulfilled in three animals (1, 4 and 6) suggesting the most effective hyperthermia treatment in these animals, whereas for animal 3 T90 was smaller (38.9°C), resulting in moderate effectiveness. The treatments for animals 2, 7 and 8 were difficult to plan due to the large tumor burden (194.0 cm^3, 912.4 cm^3, and 230.4 cm^3, respectively).

Corresponding values of T90 and ΔT indicate, only partial tumor heating to 41°C and higher and rather inhomogeneous tumor temperatures. Despite the inhomogeneity of the treated animal group, a correlation is apparent when comparing clinical responses with the predictions from planning. With the aim of having an indicative metric of the effectiveness of the treatment plans, the ratio of these volumes has been correlated with T90 from Table 2. Figure 5 shows the correlation between T90 inside the tumor from planning and the percentage of tumor volume which remained after treatment. The graph includes the original volume for each animal patient. Improved clinical responses are expected for those animals in which T90 is closer to 41°C (Table 2). In seven out of eight animals, a correlation between predictions from planning and clinical outcome was found. One exception is animal 5, the only treated patient with an oral malignant melanoma. This correlation does not constitute proof of a causal relationship between increased T90 dose and tumor shrinkage, as the tumor volume also correlates with both T90 and tumor shrinkage and thus constitutes a confounding variable. The increased tumor shrinkage could thus be related to increased heatability of small tumors, or to increased responsiveness, or to unknown additional factors. Due to the small and heterogeneous patient population, statistical separation of influence factors is not feasible.

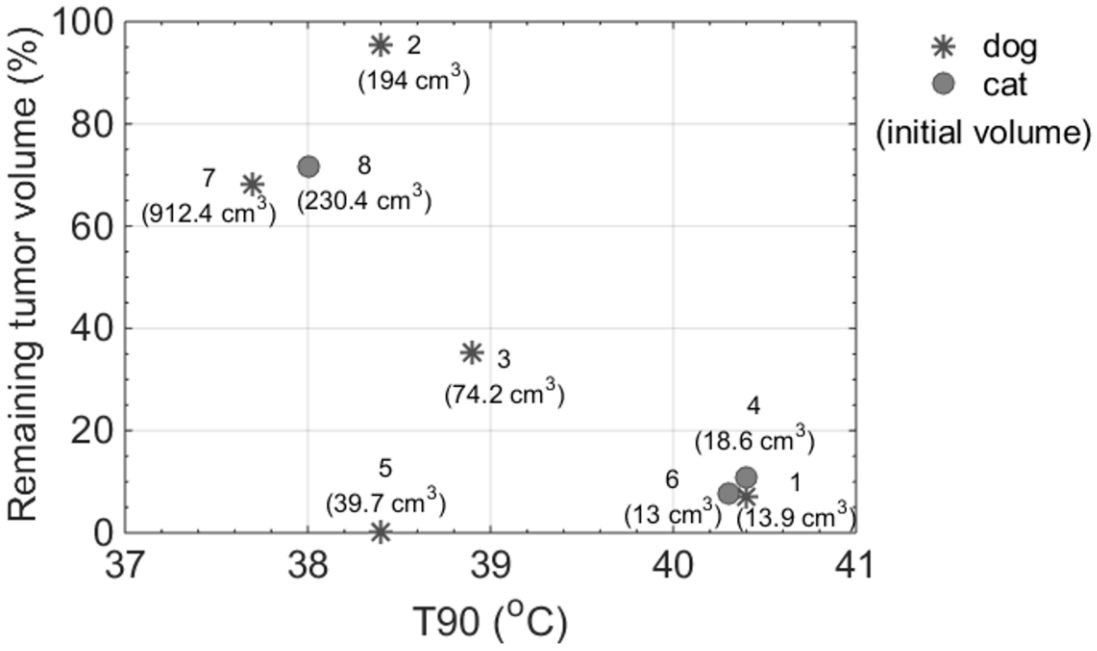

Figure 5. Remaining tumor volume after treatment versus T90 from GTV histograms for each animal patient.

Response evaluation

Median follow-up time was 283 days (range 62 – 558 days). Response was noted in each animal; time to greatest response varied from 19 to 153 days with a mean of 77 days (±47.2 days). Four animals (animal 1, 4, 5, 6) showed PR with a maximum reduction in the longest diameter ranging from 48.7 to 90.7 % with a mean of 66.7 % (±17.6 %). The remaining four animals showed SD (animal 2, 3, 7, 8); all of them had a maximum reduction in the longest diameter ranging from 4.5 to 24.2 % with a mean of 15.7 % (±8.2 %). When assessed volumetrically, a reduction in tumor volume was achieved in every case with a mean of 62.9 % (±36.6 %) based on caliper measurements. Tumor volumes and longest diameters are listed in Table 1. A modified Karnofsky´s performance grade of 0 was seen in one patient (12.5 %), grade 1 in six patients (75 %) and grade 2 in one patient (12.5 %) before therapy. During HT treatments five animals experienced five episodes of altered Karnofsky´s performance score. While four patients improved, one patient's score worsened compared to pre-treatment. During follow-up, five animals showed improved grades, one patient was recorded to worsen and two patients experienced no change towards baseline.

Of the six deceased animals, four were euthanized due to tumor-related progression causing ulceration (animal 1), bleeding (animal 2) and pain/ severe lameness (animal 8). Animal 5 showed a paraparesis of the left hind limb; further diagnostics were not performed, however metastasis of the oral melanoma could not be excluded. The other two animals (animal 3, 6) died most likely of non-tumor related causes, however necropsy was not available in these animals. Two animals were alive at the end of the study period.

In four animals additional therapy was initiated at disease progression. Metronomic chemotherapy, consisting of oral administration of cyclophosphamide (15 mg/m^2 once daily), thalidomide (2-4 mg/kg once daily) and a non-steroidal anti-inflammatory drug (piroxicam or firocoxib using the recommended standard dose)[29] was initiated. In animal 5 metronomic chemotherapy was discontinued after 151 days due to massive disease progression and oral Temozolomide was administered once daily for five consecutive days at a dosage of 60 mg/m^2 every 28 days.[30] The dog received two such cycles until treatment was discontinued and the dog euthanized due to disease progression. (Table 1)

Side effects (toxicity)

Acute thermal side effects were seen in one animal (animal 1). The dog was in slight pain (increase in heart-, and respiratory rate during anesthesia, degree I) and developed a mild erythema in the area of the treated skin (degree II). The treatment was continued with a power reduction and symptoms resolved spontaneously after the treatment (Table 1). No subacute or late thermal side effects were observed in any of the animals. Radiation toxicity was mild and not more severe than previously described for the same radiation protocol:[29] grade 1 acute toxicity of the skin was seen in seven animals (alopecia/epilation, erythema or dry desquamation) and/or in the mucous membranes (injection of the mucous membranes without mucositis) and grade 2 acute toxicity was present in the skin of one animal (patchy moist desquamation, without edema). Mild late side effects were seen in five animals with grade 1 toxicity including alopecia or leukotrichia. Transponder-related side effects were seen in two cases. In one case (animal 3), one of two transponders was expelled nine days after the placement causing a non-healing wound. No hyperthermia treatment was applied up to this time. In the second case (animal 7), three transponders were placed intra-tumorally, all of them stayed at the implanted site, however at one access/ incision site the skin did not heal, causing ulceration of the tumor. Both animals received the combined treatment as planned, but nonetheless needed surgical management afterwards. This included a debridement in the first case and a debulking of the tumor in the second case.

Thermal dose calculations

Of the 24 performed HT sessions, transponder readings from different locations could be evaluated during each treatment: temperature data was available (1) from three transponders for five treatments, (2) from two transponders for 14 treatments, and (3) from a single transponder for five treatments. The dose concepts $CEM43$ (equivalent heating duration in minutes at 43°C), Λ_{max} (largest amount of damaged repair protein) and Λ_{gap} (amount of damaged repair protein at the time of irradiation) were calculated for those 48 temperature data time series. Mean values (±SD) of $\overline{CEM43}$ = 28.74 (±33.89), $\overline{\Lambda_{max}}$ = 0.41 (±0.32) and $\overline{\Lambda_{gap}}$ = 0.13 (±0.10) were found. Figure 6 shows scatter plots of Λ_{max} vs. $CEM43$ and Λ_{gap} vs. $CEM43$, respectively.

The Spearman rank correlation for Λ_{max} vs. *CEM*43 is ρ = 0.98 and for Λ_{gap} vs. *CEM*43 is ρ = 0.90.

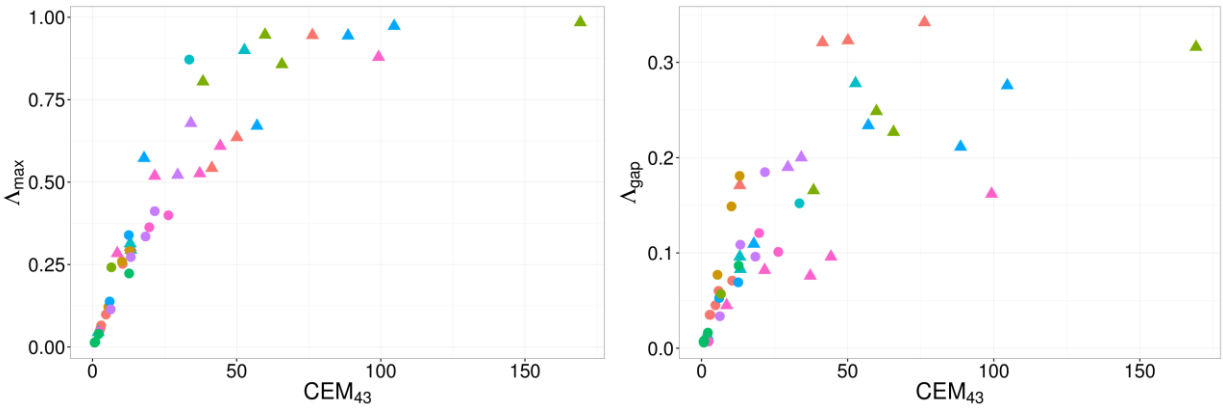

Figure 6. Scatter plot of Λ_{max} vs. CEM43 (left) and Λ_{gap} vs. CEM43 (right). Values with temperatures above 43°C are marked with a triangle. Each animal patient is assigned a distinct color.

Discussion

Prior work has proven the effectiveness of HT in combination with RT and justifies its use as an additional treatment modality in the battle against cancer.[5, 36] However, continued investigation and improvements regarding hardware and treatment planning software, as well as thermometry are mandatory to ascertain treatment quality, optimize outcome, and increase acceptance of HT as a more routine treatment option. In addition, anatomical tissue inhomogeneity with highly relevant dielectric contrast and variable tissue perfusion, intra-tumoral tissue heterogeneity, and lack of precise knowledge about the involved mechanisms (and hence the effect-related dose to be optimized) complicate the achievement of an optimal strategy for energy deposition and temperature elevation in the tumorous tissue - while avoiding overexposure of sensitive healthy tissue - and increases the demand for a mature technology.

In this study, we describe the application of an adaptive HT treatment system, preliminarily tested on a group of canine and feline cancer patients treated with three sessions of HT as an adjuvant to standard palliative RT. We further present toxicity profiles and describe clinical response in order to test the safety of the new system. Different tumor entities, locations and sizes were included, demonstrating the wide and flexible use of the hard- and software components.

In particular, large, bulky tumors have shown to challenge treatment planning in terms of achieving a homogenous temperature distribution. Temperature variations between sessions within the same animal and for the same transponders might be due to composition changes of the tumor tissue properties during or between treatments caused by altered blood supply and/or tumor shrinkage, as well as errors in reproducing the applicator positions exactly. Additionally, migration of the transponders inside the tumor between the individual HT sessions may also contribute to temperature variations since the actual measurements often do not reflect the initial, planned situation. Power adjustments were needed to achieve the aimed intra-tumoral temperatures. Despite these adaptions approximately 1/3 of measurements were out of the target range – most of them below 41°C. This fact might be explained by the rapidly raising skin temperatures under treatment, leading to a restriction of further power elevations in some cases to avoid skin damage. Nevertheless, skin temperature limits were temporarily exceeded in a few cases and in two animals almost during the entire treatment; still

none of them developed any side effects. All of the affected animals showed less than 41 *CEM*43°C in the skin, which is reported to be the thermal dose threshold for irreversible skin damage.[37, 38] The maximum *CEM*43°C reached in the skin of our animals was 30.3 *CEM*43°C.

Taking into account the heterogeneity of the treated animals, the chosen criteria for the planning-based estimation of treatment effectiveness have demonstrated good agreement with the clinical results and could be suitable as treatment optimization goals in future treatment planning. Despite the predictions for animal 5 suggesting moderate heating, results showed a reduction in tumor volume of nearly 100 %, which is consistent with previous publications of response of canine oral melanoma treated with hypofractionated RT. The reported overall response rates to RT for oral melanoma are 82 to 94 %[39] and may explain the clinical response in this case despite the moderate heating provided by HT. Cats 4 and 6, which suffered from vaccine-associated sarcoma (VAS), were supposed to have the most effective HT treatment based on the treatment planning (T90 criterion) and showed encouraging local responses with tumor volume reductions varying from 89 to 92 %. Additionally, animal 4 showed PFI of 13.3 months and was still alive at the end of data analysis. In a previous study, cats treated with a coarse fractionation RT protocol of 4 x 8 Gy for macroscopic VAS, revealed median PFI of 4 months and OS of 7 months.[40]

The thermoradiotherapy protocol used here was well tolerated by the animal patients. Apart from a single negligible acute HT toxicity that resolved spontaneously after treatment, no thermal damage was seen in any of the animals. Acute radiation side effects were mild and easily manageable and evident late radiation side effects, assessed during the follow-up period, were without any clinical relevance. Although overall treatment time and therefore time of anesthesia was longer than expected, animals were able to cope with prolonged therapy well without notable adverse effects. For low thermal doses, both scatter plots in figure 6 show a mostly linear correspondence between the C$EM43$ figure and the new thermal dose equivalent candidates Λ_{max} and Λ_{gap}. For higher thermal doses, both Λ figures are driven into saturation since the maximum of 1 (100 % of the repair protein are non-functional) cannot be exceeded. The spread in the Λ_{gap} plot is larger than in the Λ_{max} since additional variation is introduced by the differences in time-gaps. As a consequence, the correlation between Λ_{gap} and *CEM*43 is lower than between Λ_{max} and *CEM*43. No clustering around animals

and/or fraction of individual patients was observed, suggesting that the different HT sessions of a given animal were quite diverse and that the temperature inside the tumor was inhomogeneous. Interestingly, such patterns have also been observed in a study in which humans with bladder cancer were treated with the BSD-2000 system.[41] Comparing the clinical outcome with the thermal dose figures is challenging at this point due to the high variability and the low number of patients. So far, no clear trend is visible in this regard, although the reduction in the longest diameter seems to be elevated at high *CEM*43 and Λ_{max} figures. This tendency is not visible in Λ_{gap}. An aggravating factor is that the model uses the same E_a and κ regardless of whether the temperature is above or below 43°C. The computed Λ figures are therefore not accurate for sessions in which the temperature exceeded 43°C.

One main limitation of the study was related to the thermometry used during treatment. Due to the limited range of the reading device, temperature readouts required moving the applicator(s) and thus interruptions of the heating period, leading to a temperature drop and an extension of the overall treatment time. While the impact on therapeutic temperatures can be minimized by fast measurements, the frequency of measurements and the number of measuring points remains limited. Furthermore, the manual movement of the applicator and the lack of an individualized applicator holder carries the risk of positioning variations with respect to the target volume and thereby potentially altering the energy deposition. Despite this, the alterations experienced remained minimal and did not negatively influence the heating period. However, novel thermometry approaches should be considered to increase the number and rate of temperature measurements while avoiding disruptions of the heating process. Although the transponders are equipped with an anti-migration device and were placed in viable tumor areas under CT guidance, movement within the tumorous tissue was still evident and partly complicated readout and interpretation. One of the implanted transponders was rejected before the treatment start. Another animal had to be excluded from the study population, since no intra-tumoral temperature measurements were available. In a third case all injected transponders stayed at the implanted site, however at one access/incision site the skin did not heal, causing ulceration of the tumor. Further surgical intervention was needed in two of these cases, which included a debridement and debulking of the neoplasia, respectively. In these animals the tumor seemed rather active and

inflamed and the skin was fragile due to the increased tension that was created by the tumor burden itself and in one case additionally by the pre-treatment with RT. To prevent transponder-related adverse events, incision sites must be chosen in healthy skin regions overlying the tumor, however uncertain tissue characteristics and individual variations in tumor composition during treatment are unpredictable factors for therapy preparations. Additionally, tumor shrinkage during treatment suggests a need for re-optimization (currently not performed) of the HT administration to compensate for changes observed between HT sessions. The study subjects' heterogeneity regarding animal species, tumor types, sizes, and locations makes direct correlations between individual treatments difficult, but gives an indication of the wide applicability of the treatment modality and system. Moreover, it should be noted that all presented animals and tumors were treated, without treatment planning-based preselection, reflecting expected heatability.

Conclusion

In conclusion, our study shows that the novel HT system provides individually adaptive, flexible and safe HT treatments using a patient-specific treatment-planning tool and a closed-loop feedback control system to ensure that the applied treatment corresponds to predictions. All but one animals experienced improved quality of life in a palliative-intent treatment setting. Response cannot be an endpoint due to the limited number of heterogeneous cases, however the study provides a proof of principle that effective, homogenous heating can be planned and verified.

Future work should focus on image-based systems enabling re-planning and adaption of the treatment plans shortly before each session based on the current anatomical and physiological conditions to consider anatomical changes during therapy. In the future, and considering the lessons learned in the treatment of these first animals, computational planning should also be used to select patients and decide on the suitability of providing HT treatment.

Table 1. Summary of patient data, treatment, toxicity and outcome of all eight animals treated with hyperthermia and radiation therapy

Animal	Breed	Age [years]	Weight [kg]	Tumor type Location	TNM stage	Pre-treatment TV [cm^3] LD [cm]	RT protocol [Gray]	Post-treatment TV [cm^3] LD [cm]	Best RECIST[a] response	RT toxicity[b] [grade]	HT toxicity[c] [degree]	PFI [days]	Additional treatment	OS [days]
1	Irish Red and White Setter	9.9	35.4	PVWT Right lateral elbow	T1 N0 M0	13.9 5.8	12 x 3	1.0 2.2	PR	Acute: 1 Late: 0	Acute: I-II Subacute: 0 Late: 0	238	Retreatment after 481 days	558
2	English Bulldog	6.0	29.0	HSA Left inguinal	T2 N1 M0	194 10.0	5 x 6	185.2 8.3	SD	Acute: 1 Late: 0	Acute: 0 Subacute: 0 Late: 0	120	Metronomic chemo	264
3	Boxer	11.4	29.5	PVWT Right carpus	T2a N0 M0	74.2 6.6	3 x 5	26.2 5.0	SD	Acute: 1 Late: 1	Acute: 0 Subacute: 0 Late: 0	153	Debridement Metronomic chemo	220
4	Domestic short-haired cat	15.6	3.1	VAS Interscapular	T1 N0 M0	18.6 5.2	5 x 6	2.0 1.8	PR	Acute: 1 Late: 1	Acute: 0 Subacute: 0 Late: 0	400		540*
5	Rottweiler	14.8	30.0	OMM Left mandible	T3 N1 M0	39.7 5.4	4 x 8	0.1 0.5	PR	Acute: 1 Late: 1	Acute: 0 Subacute: 0 Late: 0	178	Metronomic chemo Temozolomide (2 cycles)	360
6	Domestic short-haired cat	15.5	4.9	VAS Right abdominal wall	T1 N0 M1	13.0 3.9	5 x 6	1.0 2.0	PR	Acute: 1 Late: n.a.	Acute: 0 Subacute: n.a. Late: n.a.	76	Metronomic chemo	76
7	Labrador Retriever	11.3	36.6	PVWT Right popliteal	T2a N0 M0	912.4 20.5	5 x 6	623.1 17.0	SD	Acute: 2 Late: 1	Acute: 0 Subacute: 0 Late: 0	38	Debulking	302*
8	Domestic short-haired cat	12.4	5.5	VAS Right scapula	T2b N0 M0	230.4 11.0	5 x 6	164.9 10.5	SD	Acute: 1 Late: n.a.	Acute: 0 Subacute: n.a. Late: n.a.	50		62

PVWT, perivascular wall tumor; HSA, hemangiosarcoma; VAS, vaccine-associated sarcoma; OMM, oral malignant melanoma; TV, tumor volume; LD, longest diameter measured by caliper; Best response, maximum reduction in LD; PR, partial remission; SD, stable disease; RT, radiation therapy; HT, hyperthermia; n.a., not assessable; PFI, Progression free interval; OS, Overall survival; *, censored, still alive

[a] Characterization of response according to RECIST (v1.0)

[b] Radiation toxicity criteria according to VRTOG

[c] Classification of hyperthermia-specific side effects according to CTCAE v4.03 and QMHT

Table 2. Hyperthermia treatment parameters of all eight animals

Animal	Treatment planning						Intra-tumoral temperatures during hyperthermia					
	Histogram in tumor						Transponder A		Transponder B		Transponder C	
	T90 from histogram	T10 from histogram	ΔT	Number of applicators	Initial power	Bolus temperature	Minimum	Maximum	Minimum	Maximum	Minimum	Maximum
	[°C]	[°C]	[°C]		[W]	[°C]	[°C]	[°C]	[°C]	[°C]	[°C]	[°C]
1	40.4	44.2	3.8	1	5.0	40	39.4	44.8	42.0	44.8		
							39.2	41.2	40.6	43.2		
							40.0	42.0	40.1	43.1		
2	38.4	42.6	4.2	1	5.5	38	39.1	43.4	42.0	43.3	40.3	42.0
							40.0	41.5	39.6	45.0	40.2	42.5
							39.1	41.4	41.9	43.3	40.3	41.2
3	38.9	42.4	3.5	1	2.0	41	41.7	42.6	Lost			
							41.2	42.4				
							41.3	41.8				
4	40.4	43.0	2.6	1	4.0	40	Not readable		40.8	42.6	41.8	42.8
							42.9	44.2	41.6	43.2	42.2	43.2
							41.0	43.8	39.2	40.8*	39.5	43.2
5	38.4	43.8	5.4	1	5.0	40	38.8	43.6	40.1	43.0		
							41.3	44.8	40.6	45.3		
							42.0	43.4	39.4	41.9		
6	40.3	43.6	3.3	1	5.5	41	42.2	45.7	42.3	44.1		
							Not readable		39.0	42.8		
							42.0	44.2	41.7	44.2		
7	37.7	43.4	5.7	3	5.5 each	30	39.5	40.3*	Not readable		39.4	40.2*
							Not readable		Not readable		39.2	40.2*
							Not readable		41.2	42.3	39.6	40.9*
8	38.0	43.4	5.4	2	4.5 each	40	40.8	41.8	Not readable		41.6	42.5
							41.0	42.3	Not readable		41.4	43.2
							41.7	43.6	Not readable		41.5	42.8

T90, minimum temperature reached by 90% of the tumor volume; T10, minimum temperature reached by 10% of the tumor volume; ΔT=T10-T90; Lost, transponder not available during treatment; Not readable, limited readability of the transponder during treatment; *, aimed temperature of ≥41°C not reached

References

1. Hall EJ and Giaccia AJ. Chapt. 28: Hyperthermia. In: *Radiobiology for the Radiologist*, 7th edn., Philadelphia, Lippincott Williams & Wilkins, 2012: 490-511.
2. Wust P, Hildebrandt B, Sreenivasa G, Rau B, Gellermann J, Riess H, Felix R and Schlag PM. Hyperthermia in combined treatment of cancer. *Lancet Oncol*. 2002; **3**(8): 487-97.
3. Horsman MR and Overgaard J. Hyperthermia: a potent enhancer of radiotherapy. *Clin Oncol (R Coll Radiol)*. 2007; **19**(6): 418-26.
4. Palazzi M, Maluta S, Dall'Oglio S and Romano M. The role of hyperthermia in the battle against cancer. *Tumori*. 2010; **96**(6): 902-10.
5. Cihoric N, Tsikkinis A, van Rhoon G, Crezee H, Aebersold DM, Bodis S, Beck M, Nadobny J, Budach V, Wust P and Ghadjar P. Hyperthermia-related clinical trials on cancer treatment within the ClinicalTrials.gov registry. *Int J Hyperthermia*. 2015; **31**(6): 609-14.
6. Overgaard J. The heat is (still) on--the past and future of hyperthermic radiation oncology. *Radiother Oncol*. 2013; **109**(2): 185-7.
7. Overgaard J. The current and potential role of hyperthermia in radiotherapy. *Int J Radiat Oncol Biol Phys*. 1989; **16**(3): 535-49.
8. Dewhirst MW. Animal modeling and thermal dose. *Radiol Clin North Am*. 1989; **27**(3): 509-18.
9. van der Zee J. Heating the patient: a promising approach? *Annals of Oncology*. 2002; **13**(8): 1173-84.
10. Neufeld E. High resolution hyperthermia treatment planning, Hartung-Gorre Verlag Konstanz, 2008.
11. Van de Kamer JB, Lagendijk JJ, De Leeuw AA and Kroeze H. High-resolution SAR modelling for regional hyperthermia: testing quasistatic zooming at 10 MHz. *Phys Med Biol*. 2001; **46**(1): 183-96.
12. Canters RA, Paulides MM, Franckena MF, van der Zee J and van Rhoon GC. Implementation of treatment planning in the routine clinical procedure of regional hyperthermia treatment of cervical cancer: an overview and the Rotterdam experience. *Int J Hyperthermia*. 2012; **28**(6): 570-81.
13. Paulides MM, Bakker JF, Hofstetter LW, Numan WC, Pellicer R, Fiveland EW, Tarasek M, Houston GC, van Rhoon GC, Yeo DT and Kotek G. Laboratory prototype for experimental validation of MR-guided radiofrequency head and neck hyperthermia. *Phys Med Biol*. 2014; **59**(9): 2139-54.
14. Paulides MM, Bakker JF, Neufeld E, van der Zee J, Jansen PP, Levendag PC and van Rhoon GC. Winner of the "New Investigator Award" at the European Society of Hyperthermia Oncology Meeting 2007. The HYPERcollar: a novel applicator for hyperthermia in the head and neck. *Int J Hyperthermia*. 2007; **23**(7): 567-76.
15. Paulides MM, Verduijn GM and Van Holthe N. Status quo and directions in deep head and neck hyperthermia. *Radiat Oncol*. 2016; **11**: 21.
16. Sapareto SA and Dewey WC. Thermal dose determination in cancer therapy. *Int J Radiat Oncol Biol Phys*. 1984; **10**(6): 787-800.
17. Scheidegger S, Fuchs HU, Zaugg K, Bodis S and Fuchslin RM. Using State Variables to Model the Response of Tumour Cells to Radiation and Heat: A Novel Multi-Hit-Repair Approach. *Computational and mathematical methods in medicine*. 2013; **2013**.
18. Rohrer Bley C, Blattmann H, Roos M, Sumova A and Kaser-Hotz B. Assessment of a radiotherapy patient immobilization device using single plane port radiographs and a remote computed tomography scanner. *Vet Radiol Ultrasound*. 2003; **44**(4): 470-5.
19. Paulides MM, Stauffer PR, Neufeld E, Maccarini PF, Kyriakou A, Canters RA, Diederich CJ, Bakker JF and Van Rhoon GC. Simulation techniques in hyperthermia treatment planning. *Int J Hyperthermia*. 2013; **29**(4): 346-57.
20. Hasgall PA, Di Gennaro F, Baumgartner C, Neufeld E, Gosselin MC, Payne D, Klingenböck A and Kuster N. IT'IS database for thermal and electromagnetic parameters of biological tissues. September 01st, 2015 edn., IT'IS Foundation, 2015.
21. Lang J, Erdmann B and Seebass M. Impact of nonlinear heat transfer on temperature control in regional hyperthermia. *IEEE Transactions on Biomedical Engineering*. 1999; **46**(9): 1129-38.

22. Murbach M, Neufeld E, Capstick M, Kainz W, Brunner DO, Samaras T, Pruessmann KP and Kuster N. Thermal Tissue Damage Model Analyzed for Different Whole‐Body SAR and Scan Durations for Standard MR Body Coils. *Magn Reson Med*. 2014; **71**(1): 421-31.
23. Laakso I and Hirata A. Dominant factors affecting temperature rise in simulations of human thermoregulation during RF exposure. *Phys Med Biol*. 2011; **56**(23): 7449.
24. Long S. Experimental study of the impedance of cavity-backed slot antennas. *IEEE Transactions on Antennas and Propagation*. 1975; **23**(1): 1-7.
25. Paulides M. Development of a clinical head and neck hyperthermia applicator, 2007.
26. ICRU I. Report 50. *Prescribing, recording and reporting photon beam therapy*. 1993.
27. ICRU I. Report 62. *Prescribing, Recording and Reporting Photon Beam Therapy (Supplement to ICRU Report 50)*. 1999.
28. Keyerleber MA, McEntee MC, Farrelly J and Podgorsak M. Completeness of reporting of radiation therapy planning, dose, and delivery in veterinary radiation oncology manuscripts from 2005 to 2010. *Vet Radiol Ultrasound*. 2012; **53**(2): 221-30.
29. Cancedda S, Marconato L, Meier V, Laganga P, Roos M, Leone VF, Rossi F and Bley CR. Hypofractionated radiotherapy for macroscopic canine soft tissue sarcoma: a retrospective study of 50 cases treated with a 5 x 6 Gy protocol with or without metronomic chemotherapy. *Vet Radiol Ultrasound*. 2016; **57**(1): 75-83.
30. Cancedda S, Rohrer Bley C, Aresu L, Dacasto M, Leone VF, Pizzoni S, Gracis M and Marconato L. Efficacy and side effects of radiation therapy in comparison with radiation therapy and temozolomide in the treatment of measurable canine malignant melanoma. *Vet Comp Oncol*. 2014.
31. Bateman KE, Catton PA, Pennock PW and Kruth SA. 0-7-21 radiation therapy for the palliation of advanced cancer in dogs. *J Vet Intern Med*. 1994; **8**(6): 394-9.
32. Chretin J, Rassnick K, Shaw N, Hahn KA, Ogilvie GK, Kristal O, Northrup NC and Moore AS. Prophylactic trimethoprim-sulfadiazine during chemotherapy in dogs with lymphoma and osteosarcoma: A double-blind, placebo-controlled study. *J Vet Intern Med.* 2007; 21: 141-148.
33. Nguyen SM, Thamm DH, Vail DM and London CA. Response evaluation criteria for solid tumours in dogs (v1.0): a Veterinary Cooperative Oncology Group (VCOG) consensus document. *Vet Comp Oncol*. 2015; **13**(3): 176-83.
34. Ladue T, Klein MK and Veterinary Radiation Therapy Oncology G. Toxicity criteria of the veterinary radiation therapy oncology group. *Vet Radiol Ultrasound*. 2001; **42**(5): 475-6.
35. Bruggmoser G, Bauchowitz S, Canters R, Crezee H, Ehmann M, Gellermann J, Lamprecht U, Lomax N, Messmer MB, Ott O, Abdel-Rahman S, Schmidt M, Sauer R, Thomsen A, Wessalowski R, van Rhoon G, Atzelsberg Research G and European Society for Hyperthermic O. Guideline for the clinical application, documentation and analysis of clinical studies for regional deep hyperthermia: quality management in regional deep hyperthermia. *Strahlenther Onkol*. 2012; **188 Suppl 2**: 198-211.
36. Januszewski A and Stebbing J. Hyperthermia in cancer: is it coming of age? *Lancet Oncol*. 2014; **15**(6): 565-6.
37. Dewhirst MW, Viglianti BL, Lora-Michiels M, Hanson M and Hoopes PJ. Basic principles of thermal dosimetry and thermal thresholds for tissue damage from hyperthermia. *Int J Hyperthermia*. 2003; **19**(3): 267-94.
38. van Rhoon GC, Samaras T, Yarmolenko PS, Dewhirst MW, Neufeld E and Kuster N. CEM43 degrees C thermal dose thresholds: a potential guide for magnetic resonance radiofrequency exposure levels? *Eur Radiol*. 2013; **23**(8): 2215-27.
39. Withrow SJ, Vail DM and Page RL. Withrow & MacEwen's small animal clinical oncology, 2013.
40. Eckstein C, Guscetti F, Roos M, Martin de las Mulas J, Kaser-Hotz B and Rohrer Bley C. A retrospective analysis of radiation therapy for the treatment of feline vaccine-associated sarcoma. *Vet Comp Oncol*. 2009; **7**(1): 54-68.
41. Scheidegger S, Füchslin RM, Timm O, Eberle B and Bodis S. A novel approach for thermal dosimetry. In: *Proc ESHO Annual Meeting 2015* edn., Zurich: European Society for Oncological Hyperthermia. , 2015: 26.

Danksagung

Ich möchte mich hiermit bei meiner Doktormutter Prof. Carla Rohrer Bley bedanken, die mir die Möglichkeit gegeben hat, diese Arbeit in ihrer Abteilung anzufertigen und mich während dieser Phase intensiv, kompetent und konstruktiv unterstützt hat.

Ein grosser Dank gilt ebenso dem ganzen Team der Abteilung für Radio-Onkologie, welches mich freundschaftlich aufgenommen hat und mich mit wertvollen Anregungen, unermüdlicher Hilfsbereitschaft und Geduld tatkräftig unterstützt hat.

Danken möchte ich ausserdem dem gesamten Hyperthermie-Netzwerkteam, allen voran der Gruppe um Prof. Stephan Bodis sowie der IT'IS Foundation, die mit ihren innovativen Ideen, ihrem Engagement sowie ihrer Diskussionsbereitschaft zu einem wesentlichen Gelingen dieser Arbeit beigetragen hat.

Besonders danken möchte ich Marcus, Constanze und Franziska für die bedingungslose Unterstützung und vielen lieben und aufbauenden Worte während der Erarbeitung meiner Dissertation.

Curriculum Vitae

Vorname Name	Susann Dressel
Geburtsdatum	01.07.1989
Geburtsort	Stollberg
Nationalität	Deutsch

07/1996 – 07/2000	**Grundschule** (Grundschule I Lugau/ Erzgeb., Deutschland)
08/2000 – 07/2005	**Gymnasium** (Gymnasium Oelsnitz/ Erzgeb., Deutschland)
08/2005 – 07/2008	**Gymnasium** (Carl-von-Bach-Gymnasium Stollberg, Deutschland)
04.07.2008	**Abitur**, Carl-von-Bach-Gymnasium Stollberg, Deutschland
10/2008 – 03/2014	**Studium der Veterinärmedizin** (Justus-Liebig-Universität Giessen, Deutschland)
27.03.2014	**Approbation als Tierärztin vet. med.** (Justus-Liebig-Universität Giessen, Deutschland)
04/2014 – 03/2017	Anfertigung der Dissertation unter Leitung von Prof. Dr. med. vet. Carla Rohrer Bley am Departement für Kleintiere, Abteilung für Radio-Onkologie der Vetsuisse-Fakultät Universität Zürich
04/2014 – 03/2017	**Assistenzärztin**, Abteilung für Radio-Onkologie, Vetsuisse Fakultät, Universität Zürich, Schweiz